infrastructures

MDPI

Article

Dynamic Probabilistic Modeling of Concrete Strength: Markov Chains and Regression for Sustainable Mix Design

Md. Shahariar Ahmed [1], Anica Tasnim [2], Md Ferdous Hasan [3] and Golam Kabir [1,*]

[1] Industrial Systems Engineering, Faculty of Engineering and Applied Science, University of Regina, 3737 Wascana Parkway, Regina, SK S4S 0A2, Canada; map028@uregina.ca
[2] Environmental Systems Engineering, Faculty of Engineering and Applied Science, University of Regina, 3737 Wascana Parkway, Regina, SK S4S 0A2, Canada; atg748@uregina.ca
[3] Department of Textile Engineering, Khulna University of Engineering & Technology, Khulna 9203, Bangladesh; mdferdous0502@gmail.com
* Correspondence: golam.kabir@uregina.ca; Tel.: +1-306-585-5271

Abstract

Concrete is fundamental to modern construction, comprising 70% of all building materials and supporting an industry projected to reach $15 trillion by 2030. Predicting compressive strength—a key factor for structural safety and resource efficiency—remains a challenge, as conventional models often fail to capture the dynamic, time-dependent nature of strength development across mix compositions and curing intervals. This study proposes an integrated modeling framework using Markov Chain analysis and regression, validated on 135 samples from 27 mixtures with varying proportions of Portland Cement (PC), Fly Ash (FA), and Blast Furnace Slag (BFS) over curing periods from 3 to 180 days. The Markov Chain framework, integrated with regression analysis, models strength transitions across 10 states (9–42 MPa), with high accuracy (R^2 = 0.977, standard error = 3.27 MPa). Curing time (β = 0.079), PC proportion (β = 0.063), and BFS proportion (β = 0.051) are identified as key drivers, while higher FA content (β = 0.019) enhances long-term durability. Model validation using Coefficient of Variation (CoV = 15.57%) and mean absolute error confirms robust and consistent performance across mix designs. The framework supports tailored mix strategies—PC for early strength, BFS for durability, FA for sustainability—empowering engineers to optimize mix selection and curing strategies for efficient and durable concrete applications.

Keywords: compressive strength; concrete mix optimization; Markov chain modeling; regression analysis; sustainability; predictive modeling

check for updates

Academic Editors: Ghasan Fahim Huseien and Iman Faridmehr

Received: 9 June 2025
Revised: 28 July 2025
Accepted: 15 August 2025
Published: 20 August 2025

Citation: Ahmed, M.S.; Tasnim, A.; Hasan, M.F.; Kabir, G. Dynamic Probabilistic Modeling of Concrete Strength: Markov Chains and Regression for Sustainable Mix Design. *Infrastructures* **2025**, *10*, 219. https://doi.org/10.3390/infrastructures10080219

Copyright: © 2025 by the authors. Licensee MDPI, Basel, Switzerland. This article is an open access article distributed under the terms and conditions of the Creative Commons Attribution (CC BY) license (https://creativecommons.org/licenses/by/4.0/).

1. Introduction

Concrete compressive strength is a fundamental property that determines the resilience and stability of structures, evolving gradually throughout the curing process [1]. This progression is driven by the material composition—particularly the proportions of Portland Cement (PC), Fly Ash (FA), and Blast Furnace Slag (BFS)—and curing duration, making accurate strength prediction vital for effective mix design, optimized material usage, and sustainable construction practices [2,3]. The environmental impact of concrete, primarily from high PC content, contributes significantly to carbon emissions, necessitating the use of SCMs like FA and BFS to reduce the PC proportion by 20–30% while maintaining or enhancing strength and durability [4]. Traditional predictive methods, such as regression analysis and neural networks, face limitations. Regression models typically achieve R^2

values of 0.80–0.85 for standard mixes but struggle with nonlinear and time-dependent effects, often yielding standard errors of 5–7 MPa for diverse mixtures [5]. Neural networks can reach R^2 values up to 0.95 but require extensive training data, lack interpretability, and are impractical for real-time mix adjustments, especially for mixes with high FA or BFS content under variable curing conditions [6,7]. These limitations underscore the need for flexible, dynamic approaches, such as Markov Chains integrated with statistical methods, to model the time-dependent evolution of concrete strength effectively.

This study aims to pioneer a hybrid modeling framework that integrates probabilistic and statistical approaches to dynamically predict concrete compressive strength, enabling adaptive mix design optimization with PC, FA, and BFS for sustainable and high-performance construction. Unlike prior studies using the same dataset for static predictions [2], this work advances dynamic strength forecasting, real-time mix adjustments, and eco-friendly design strategies, leveraging 135 samples from 27 mixes to achieve superior accuracy (R^2 = 0.977, CoV = 15.57%) and actionable insights for diverse structural applications.

The study is guided by the following research questions (RQs):

- RQ-1: How do varying proportions of PC, FA, and BFS drive the dynamic evolution of compressive strength across diverse concrete mixes, achieving superior accuracy (R^2 = 0.977) over static neural network models by modeling nonlinear material interactions?
- RQ-2: How does curing time govern compressive strength progression in PC-, FA-, and BFS-based mixes, enabling tailored curing schedules with higher precision (CoV = 15.57%) than traditional curing models?
- RQ-3: How can high-accuracy compressive strength forecasting (R^2 = 0.977) optimize mix designs for specific structural applications, such as precast or high-performance structures, offering real-time adaptability beyond less practical ML models?
- RQ-4: How can predictive modeling minimize PC use while maximizing FA and BFS contributions to enhance durability and sustainability, achieving eco-friendly designs that surpass prior deterioration-focused studies?

These RQs collectively address the need for dynamic, accurate, and sustainable concrete mix design to provide actionable insights that surpass the limitations of prior static or data-intensive methods [2,5].

2. Literature Review

2.1. Traditional Models for Strength Prediction

Traditional approaches to predicting concrete compressive strength rely on empirical formulas and regression-based models. Standards such as ACI and CEB-FIP employ simple relationships between parameters like water–cement ratio and compressive strength, typically achieving R^2 values of 0.80–0.85 for conventional mixes [3]. However, these models are limited by their linear assumptions, making them less effective for mixes incorporating supplementary cementitious materials (SCMs) such as Fly Ash (FA) and Blast Furnace Slag (BFS), or under variable curing conditions. Studies using regression and neural network models with diverse binder compositions have shown only moderate accuracy (R^2 = 0.80–0.95) and failed to capture the full time-dependent evolution of strength, especially over extended curing intervals [2,7]. Additionally, regression models often overlook nonlinear interactions and the dominant influence of curing time (β = 0.079, yielding standard errors of 5–7 MPa for non-standard mixes [5]. The static nature of these traditional models limits their capacity for adaptive mix design in modern construction environments.

2.2. Machine Learning Approaches

Machine learning (ML) models, including support vector machines, decision trees, and neural networks, have advanced the prediction of compressive strength by modeling complex interactions among binder components, curing regimes, and environmental factors. Neural networks, for example, can achieve R^2 values up to 0.95 when trained on large datasets, outperforming empirical models [1]. Despite their improved accuracy, ML approaches are computationally intensive and lack interpretability, restricting their use for real-time mix adjustments and on-site applications [6]. These methods also require extensive training data and prediction times and often fail to provide actionable recommendations for specific structural needs, such as early-strength requirements in precast concrete. The practical limitations of ML models underscore the need for dynamic, interpretable approaches that can bridge the gap between accuracy and usability.

2.3. The Influence of Material Composition, Curing Time, and Sustainability

Compressive strength development in concrete is intimately linked to binder composition and curing duration. Portland cement (PC) is essential for early strength gains (7–28 days), which are critical for rapid construction and precast applications. In contrast, FA and BFS contribute to long-term durability and sustainability, though their inclusion can delay early strength development [7]. Mixes with higher FA content often exhibit lower early strength compared to PC-rich mixes, while BFS becomes more influential at later ages, enhancing long-term compressive strength [8]. Contemporary sustainability initiatives emphasize the reduction of PC content in favor of FA and BFS, achieving significant reductions in emissions while maintaining target strength levels over time [4,8]. Previous studies have explored the potential of SCMs in mitigating deterioration and enhancing durability but have generally not integrated dynamic predictive modeling for optimized mix design. Research focused on probabilistic models for long-term performance [6] also tends to overlook the need for real-time, adaptive optimization strategies.

2.4. Research Gaps and the Current Study's Contributions

Despite substantial progress, several persistent gaps remain in the literature. Traditional models are static and linear and unable to dynamically capture the evolution of compressive strength, especially for SCM-rich mixes [2,3,7]. Machine learning approaches, although more accurate, are limited by their lack of transparency, high data requirements, and impracticality for real-time or on-site applications [1,6]. Sustainability-oriented studies emphasize SCM benefits but rarely integrate dynamic predictive frameworks for mix design optimization, often focusing on durability or deterioration rather than holistic strength development [4,5,8].

This study makes the following contributions to the literature:

- Critically synthesizes limitations of conventional and machine learning-based models for dynamic strength prediction, highlighting the need for interpretable, practical, and sustainability-oriented approaches.
- Develops a hybrid modeling framework combining Markov Chain theory and regression analysis, enabling robust, time-dependent prediction of compressive strength for diverse binder compositions and curing intervals.
- Implements validation using Coefficient of Variation (CoV), providing a normalized, literature-benchmarked measure of predictive consistency and reliability for concrete strength modeling.
- Delivers actionable, real-time recommendations for sustainable mix design, facilitating reduction of the Portland Cement proportion and enhanced use of FA and BFS, supporting environmental goals without compromising performance.

The specific work in this article is shown in Figure 1. The flowchart presents the methodology: data collection, Markov Chain state definition, regression modeling, model validation, and sustainable mix design recommendations.

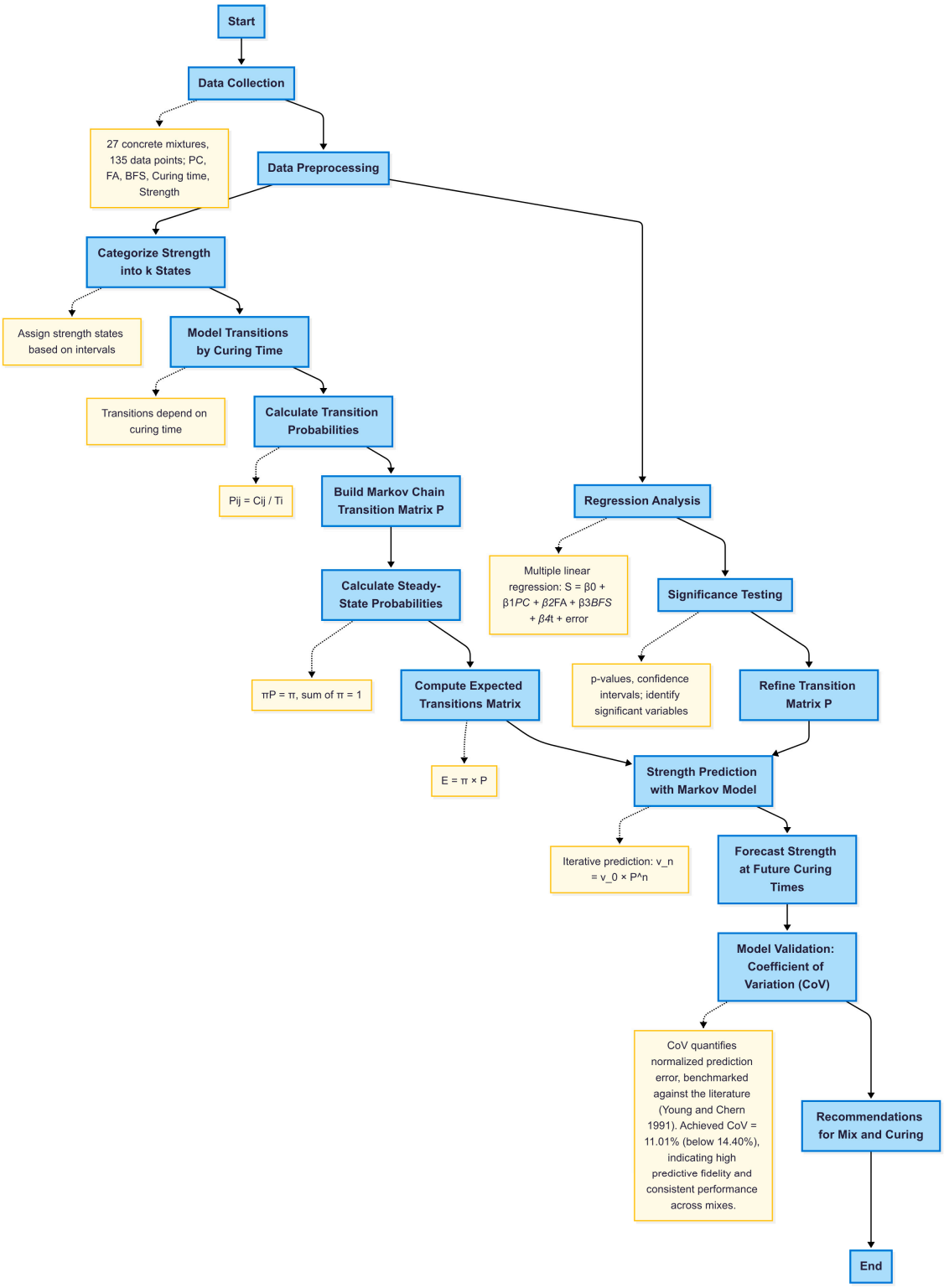


Figure 1. Flowchart of concrete compressive strength prediction: methodology overview.

3. Methodology

This integrated approach uses Markov Chain modeling and regression analysis to predict concrete compressive strength evolution across mix compositions and curing in-

tervals. Data are collected and preprocessed, strengths are categorized into discrete states, and transition probabilities capture progression. Regression analysis refines the Markov model, enabling accurate forecasting and supporting optimal mix and curing decisions. The overall methodology is depicted in the flowchart (Figure 1).

3.1. Data Collection

The dataset for this study consists of 27 unique concrete mixtures [2], each with varying proportions of Portland Cement (PC), Fly Ash (FA), and Blast Furnace Slag (BFS). Compressive strength measurements were taken at five curing intervals (3, 7, 28, 90, and 180 days) for each mixture, resulting in 135 data points. Each data point includes:

- Mix Code (M_i): identifier for each mixture, such as $C_{ontrol,}$ M_1, M_2 etc.
- PC, FA, BFS composition (kg/m^3) (x_{PC}, x_{FA}, x_{BFS}): quantities of each material used per cubic meter.
- Curing time (t): the curing period in days for each measurement.
- Compressive strength (S): measured compressive strength in MPa.

All specimens were cured under controlled ambient conditions (20 ± 2 °C, 65 ± 5% RH), strictly following the original experimental protocol [2]. This standardized approach ensures consistency across mixtures and aligns with established research practices. The resulting dataset enables detailed analysis of strength evolution across curing periods and binder compositions, serving as the foundation for Markov Chain modeling (Appendix A Table A1).

A key strength of the methodology is the deliberate variation in binder composition—specifically the proportions of PC, BFS, and FA—which serves as the primary independent variable. This diversity enables robust evaluation of how different binder systems influence strength development, offering valuable insights for mixed optimization and sustainable design. Rather than limiting analysis, the range of binder systems enhances the model's applicability to real-world concrete practices. Results are interpreted within the context of binder chemistry, supporting informed recommendations for tailored, durable, and environmentally conscious mix designs.

While the dataset includes compressive strengths below 20 MPa, this inclusive range supports rigorous model calibration and broadens the analytical perspective. Importantly, the proposed framework is fully extensible to higher strength regimes, including those required for structural and high-performance concrete. This versatility ensures relevance for both standard and advanced applications and positions the model for future expansion in alignment with international engineering standards and evolving industry demands.

3.2. Data Preprocessing

The raw data underwent several preprocessing steps to prepare it for Markov Chain analysis.

3.2.1. Categorization of Strength States

Each compressive strength value (S: 9–42 MPa; Table A1) was classified into one of ten discrete states (S1–S10) using ~2.5–3.3 MPa intervals derived from histogram analysis of the 135 data points. Open-ended bounds were applied to State 1 (<13.5 MPa) and State 10 (>33.5 MPa) [8]. This ten-state system ensures robust transition counts [9] and aligns with practical use: States 1–3 for early strength, 4–6 for general construction, and 7–10 for high-performance concrete [10]. The intervals also align with the regression model's standard error (3.27 MPa). A mix is denoted as Mi (t), e.g., M3 (3,7) for mix M3 at 3 and 7 days. Table 1 summarizes states, MPa ranges, and corresponding mix codes with curing ages.

Table 1. Compressive strength ranges and associated mixes with state numbers.

State	Compressive Strength Range (MPa)	Mix Code and Curing Age M_i (t)
State 1	<13.5	M3 (3, 7), M5 (60), M9 (90), M10 (0), M12 (60), M13 (90), M14 (120), M20 (150), M23 (60), M25 (120), M26 (150), M27 (180)
State 2	13.5–16	M3 (7), M4 (3, 7), M6 (0), M7 (30), M8 (60), M9 (90), M10 (0), M11 (30), M12 (60), M13 (90), M14 (120), M19 (120), M21 (0), M22 (30), M24 (90)
State 3	16–18.5	M2 (3, 7), M3 (28), M4 (28), M6 (0), M7 (30), M8 (60), M9 (90), M10 (0), M11 (30), M12 (60), M13 (90), M14 (120), M17 (60), M18 (90), M19 (120), M20 (150), M21 (0), M22 (30), M24 (90)
State 4	18.5–21	M1 (28), M2 (28), M4 (7), M5 (60), M6 (0), M8 (60), M9 (90), M10 (0), M11 (30), M12 (60), M13 (90), M14 (120), M15 (0), M16 (30), M17 (60), M19 (120), M20 (150), M22 (30), M23 (60), M24 (90)
State 5	21–23.5	M1 (90), M2 (180), M3 (90), M4 (90), M5 (60), M6 (0), M8 (60), M9 (90), M10 (0), M11 (30), M12 (60), M13 (90), M15 (0), M16 (30), M17 (60), M19 (120), M20 (150), M23 (60), M24 (90), M25 (120), M26 (150)
State 6	23.5–26	M1 (180), M2 (180), M3 (180), M4 (180), M5 (60), M7 (30), M8 (60), M9 (90), M10 (0), M11 (30), M12 (60), M13 (90), M14 (120), M15 (0), M16 (30), M17 (60), M18 (90), M19 (120), M20 (150), M23 (60), M24 (90), M25 (120), M26 (150)
State 7	26–28.5	M1 (90), M2 (180), M3 (180), M5 (60), M6 (0), M7 (30), M8 (60), M9 (90), M10 (0), M11 (30), M12 (60), M13 (90), M14 (120), M15 (0), M16 (30), M17 (60), M18 (90), M19 (120), M20 (150), M22 (30), M23 (60), M24 (90), M25 (120), M26 (150)
State 8	28.5–31	M3 (180), M5 (60), M6 (0), M7 (30), M8 (60), M9 (90), M10 (0), M11 (30), M12 (60), M13 (90), M14 (120), M15 (0), M16 (30), M17 (60), M18 (90), M19 (120), M20 (150), M22 (30), M23 (60), M24 (90), M25 (120), M26 (150)
State 9	31–33.5	M1 (90), M2 (180), M3 (180), M5 (60), M6 (0), M7 (30), M8 (60), M9 (90), M10 (0), M11 (30), M12 (60), M13 (90), M14 (120), M15 (0), M16 (30), M17 (60), M18 (90), M19 (120), M20 (150), M23 (60), M24 (90), M25 (120), M26 (150)
State 10	>33.5	M1 (90), M3 (180), M4 (180), M5 (60), M6 (0), M7 (30), M8 (60), M9 (90), M10 (0), M11 (30), M12 (60), M13 (90), M14 (120), M15 (0), M16 (30), M17 (60), M18 (90), M19 (120), M20 (150), M22 (30), M23 (60), M24 (90), M25 (120), M26 (150)

3.2.2. Curing-Time-Driven Transition State and Probability Modeling

The analysis in this study focuses on immediate transitions between states, driven by changes in curing time. The transition probability P_{ij} is calculated using the following formula:

$$P_{ij} = \frac{C_{ij}}{T_i}, \; T_i = \sum_j C_{ij} \tag{1}$$

where

- P_{ij} is the probability of transitioning from state S_i to state S_j;
- C_{ij} is the count of transitions observed from state S_i to state S_j (this represents the number of times the system moved directly from state S_i to state S_j in the observed dataset);
- T_i is the total number of transitions originating from state S_i (it is calculated by summing all the transitions from S_i to any other state, i.e., the total number of transitions starting from state S_i to any state S_j).

Example: Let us consider a dataset where we observe transitions between different states. Suppose we have the following data for State 1. The transition probability from State 1 to State 2 is as follows:

$$P(S_1 \rightarrow S_2) = \frac{C_{12}}{T_1} = \frac{10}{17} \approx 0.588$$

Thus, based on the dataset, the transition probability from State 1 to State 2 is approximately 0.588, or 58.8%. Further details are provided in Appendix A Table A2.

3.3. Markov Chain Model Development

The Markov Chain model was constructed to forecast compressive strength transitions as the concrete cures.

3.3.1. Transition Matrix Construction

The transition probabilities between states were calculated to form the Markov Chain transition matrix P (Table 2). For states S_i and S_j, the transition probability pij represents the likelihood of moving from state S_i at time t to state S_j at time $t + 1$, resulting in a $k \times k$ matrix P with elements p_{ij} such that $\sum_{j=1}^{k} p_{ij} = 1$ for all i.

Table 2. Transition probability matrix.

From/To	State 1	State 2	State 3	State 4	State 5	State 6	State 7	State 8	State 9	State 10
State 1	0.176	0.588	0.176	0.059	0.000	0.000	0.000	0.000	0.000	0.000
State 2	0.000	0.227	0.545	0.227	0.000	0.000	0.000	0.000	0.000	0.000
State 3	0.000	0.000	0.231	0.231	0.192	0.269	0.077	0.000	0.000	0.000
State 4	0.000	0.000	0.067	0.133	0.400	0.200	0.200	0.000	0.000	0.000
State 5	0.154	0.000	0.000	0.000	0.077	0.308	0.000	0.308	0.077	0.077
State 6	0.125	0.063	0.063	0.000	0.000	0.125	0.250	0.313	0.063	0.000
State 7	0.200	0.300	0.000	0.000	0.000	0.000	0.100	0.200	0.200	0.000
State 8	0.545	0.091	0.182	0.000	0.000	0.000	0.000	0.000	0.091	0.091
State 9	0.000	0.400	0.200	0.200	0.000	0.000	0.000	0.000	0.000	0.200
State 10	0.500	0.000	0.000	0.250	0.000	0.000	0.000	0.000	0.000	0.250

3.3.2. Steady-State Calculations

To understand the long-term behavior of the system, the steady-state probabilities π for each strength state were calculated using the following equation.

$$\pi \mathrm{P} = \pi, \sum_{i=1}^{k} \pi_i = 1 \quad (2)$$

where π_i represents the steady-state probability of the strength remaining in or reaching state S_i. This steady-state distribution helps in identifying the expected compressive strength distribution if curing were to continue indefinitely (Table 3).

Table 3. Steady-state probability distribution.

State	State 1	State 2	State 3	State 4	State 5	State 6	State 7	State 8	State 9	State 10
Probability	0.1207	0.1575	0.1865	0.1156	0.0889	0.1151	0.0736	0.078	0.0358	0.0281

3.3.3. Expected Transitions Matrix

The expected transitions matrix combines the steady-state distribution and the transition matrix to forecast how frequently transitions will occur between states over time. This matrix is calculated as follows:

$$E = \pi \times P \tag{3}$$

where E is the expected transitions matrix; π is the steady-state distribution, representing the long-term probability of being in each state; and P is the transition matrix, representing the probability of transitioning from one state to another.

3.4. Regression Analysis

A regression model was employed to validate the effects of composition and curing time on compressive strength, thereby supporting the accuracy of the Markov Chain predictions.

3.4.1. Model Structure

A multiple linear regression model was developed with compressive strength S as the dependent variable and the mixture components (x_{PC}, x_{FA}, x_{BFS}) and curing time t as independent variables:

$$S = \beta_0 + \beta_1 x_{PC} + \beta_2 x_{FA} + \beta_3 x_{BFS} + \beta_4 t + \epsilon \; P \tag{4}$$

where β_i are the coefficients representing the impact of each variable and ϵ is the error term. The coefficients β_i were estimated using least-squares estimation.

3.4.2. Significance Testing

The regression model was analyzed for statistical significance, with p-values and confidence intervals calculated for each β_i to determine the influence of each variable on compressive strength. Variables with $p < 0.05$ were considered statistically significant, indicating strong influence on strength transitions.

3.4.3. Model Refinement

In addition to validating variable importance, regression analysis directly informs and refines the Markov Chain modeling by translating the statistical influence of mix components and curing time into the transition probabilities between strength states. The regression coefficients for PC (0.063), FA (0.019), BFS (0.051), and curing time (0.079), all with high statistical significance, quantify how each factor drives compressive strength development across the dataset. Instead of relying only on observed transition counts, the Markov transition matrix is recalibrated using these regression insights—mixes with higher BFS or longer curing receive greater probabilities for reaching advanced strength states, while early transitions for high-FA mixes are reduced. Predicted strengths for each mix and curing interval from the regression model guide the adjustment of transition probabilities, ensuring the Markov Chain remains sensitive to actual material effects and curing behaviors. For instance, mixes such as M16 (high BFS, long curing; actual 42 MPa, regression 45 MPa) are assigned higher probabilities for reaching top strength states, while M14 (high FA, short curing; actual 10 MPa, regression 15 MPa) is less likely to show early strength gains. This data-driven refinement allows the Markov model to more accurately forecast compressive strength evolution for different mix designs.

3.4.4. Model Validation

Model validation was performed by directly comparing the predicted compressive strength values against the experimentally measured data for all concrete mixtures and curing intervals. In this study, the entire dataset was utilized for both model development and validation, as illustrated in Figure 1. This approach was chosen to maximize the robustness of parameter estimation, given the available sample size and the variability across mixtures and curing times. The predictive performance of both the regression and Markov Chain models was evaluated using statistical metrics, including coefficient of determination (R^2), root mean square error (RMSE), and standard error. These metrics provide a quantitative assessment of the goodness of fit and the accuracy of the models in forecasting concrete compressive strength throughout the full range of experimental conditions. Graphical analysis, such as scatter plots and regression lines, further illustrate the relationship between predicted and actual values, supporting the reliability and interpretability of the modeling approach.

In addition to standard regression metrics, further model validation was conducted using the Coefficient of Variation (CoV), a benchmark error metric widely employed in concrete strength modeling. The CoV provides a normalized measure of prediction error relative to the mean observed strength, enabling direct comparison to the established literature standards [11]. This approach offers an additional layer of statistical rigor, ensuring that the predictive accuracy of the integrated regression–Markov model is consistent across a diverse range of mix designs and curing intervals.

3.5. Strength Prediction Using the Markov Chain Model

By applying the Markov Chain model iteratively across curing intervals, the likelihood of each strength state at future curing times was calculated. For an initial state vector v_0 [0.5185, 0.3333, 0.0370, 0.0741, 0.0370, 0.0, 0.0, 0.0, 0.0, 0.0], representing the starting strength distribution, the future distribution after n steps (days) is given by the following:

$$v_n = v_0 P^n \cdot P \tag{5}$$

where P^n is the n-step transition matrix. This prediction enabled forecasting compressive strength at each curing stage and provided recommendations for optimal mixture compositions and curing schedules based on the projected state transitions.

4. Results

4.1. Steady-State Transitions and Markov Chain Analysis

The probability distributions provide insight into the likelihood of transitioning between different compressive strength states (State 1 to State 10) are presented in Figure 2.

State 1 (11.0–13.5 MPa): State 1 represents the lowest strength range, with a steady-state probability of 12.07%. This aligns with early stage curing behaviors, often observed in mixes with low Portland Cement content or those underperforming during the initial curing phase. These mixtures exhibit limited early strength development, emphasizing the need for adjustments in material composition or curing methods to accelerate the initial strength gain.

State 2 (13.5–16.0 MPa): State 2 has a steady-state probability of 15.75%, indicating that as curing progresses, many mixtures transition into this range. This corresponds to early to mid-stage curing, where concrete gains moderate strength, striking a balance between underperformance and early strength development. This state often reflects mixes optimized for gradual strength progression in the early curing phases.

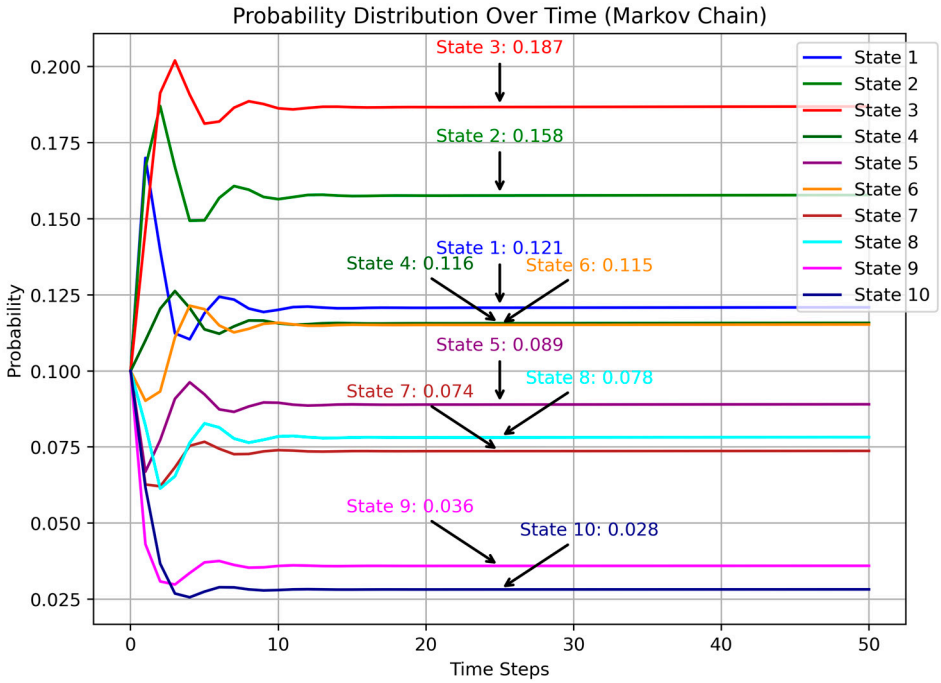


Figure 2. Probability distributions over time (Markov Chain).

State 3 (16.0–18.5 MPa): State 3, with a steady-state probability of 18.65%, marks a significant range for mixes achieving balanced strength development during curing. These mixtures often consist of a well-proportioned combination of Portland Cement and Fly Ash, allowing steady strength gains. State 3 is ideal for standard construction applications requiring moderate compressive strength early in the curing process.

State 4 (18.5–21.0 MPa): State 4 has a steady-state probability of 11.56% and represents mid-stage curing, suitable for moderate structural applications. Mixtures in this state exhibit consistent strength progression, reflecting balanced material compositions that support stability and durability for non-critical elements in construction.

State 5 (21.0–23.5 MPa): State 5 occurs less frequently, with a probability of 8.89%, indicating the need for optimized designs or extended curing to achieve this strength. This state is associated with mixes requiring enhanced curing protocols, often tailored for moderate to high structural applications that demand reliable compressive strength.

State 6 (23.5–26.0 MPa): State 6, with a steady-state probability of 11.51%, marks the transition to higher strength levels suitable for demanding structural elements. This range emphasizes well-balanced curing methods and material compositions, particularly for mixes with higher Portland Cement or Blast Furnace Slag content, designed for applications requiring significant load-bearing capacity.

State 7 (26.0–28.5 MPa): State 7 has a low steady-state probability of 7.36%, indicating that only a small proportion of mixtures achieve this range during curing. These mixtures typically require high Portland Cement content or special curing techniques to enhance strength. State 7 is suitable for high-stress applications, with careful monitoring needed to ensure consistent performance.

State 8 (28.5–31.0 MPa): State 8, with a steady-state probability of 7.80%, represents high-strength concrete achieved through prolonged curing or specialized methods. Mixes in this range often include a higher proportion of Blast Furnace Slag or Portland Cement and are designed for heavy-load structural components.

State 9 (31.0–33.5 MPa): State 9 has a very low steady-state probability of 3.58%, highlighting that only a small number of mixtures reach this strength level. These mixes are

typically utilized in high-performance applications, such as critical infrastructure, and often involve sophisticated curing methods or special additives to meet the required strength.

State 10 (33.5–36.0 MPa): State 10 represents the peak strength range, with the lowest probability of 2.81%. This range is typically achieved in high-performance concrete designed for critical applications like bridges or high-rise buildings. These mixes require controlled environments and advanced curing techniques to ensure their exceptional strength and durability.

4.2. Transition Matrix Analysis

4.2.1. Dynamic Strength Evolution Through Markov Chain Analysis

The Markov Chain analysis offers a dynamic view of how concrete compressive strength evolves over curing time. Each state corresponds to a defined strength range, from State 1 (11.0–13.5 MPa) to State 10 (33.5–36.0 MPa). Transition probabilities illustrate the likelihood of strength progression between states (Figure 3). For example, early-stage mixes in State 1 show a 71% chance of transitioning to State 2, reflecting minor strength increases, while State 2 mixes exhibit an 85.9% probability of advancing to State 3, signifying rapid strength gains. These trends highlight the influence of composition, such as Portland Cement (PC) and Fly Ash (FA), on the curing process.

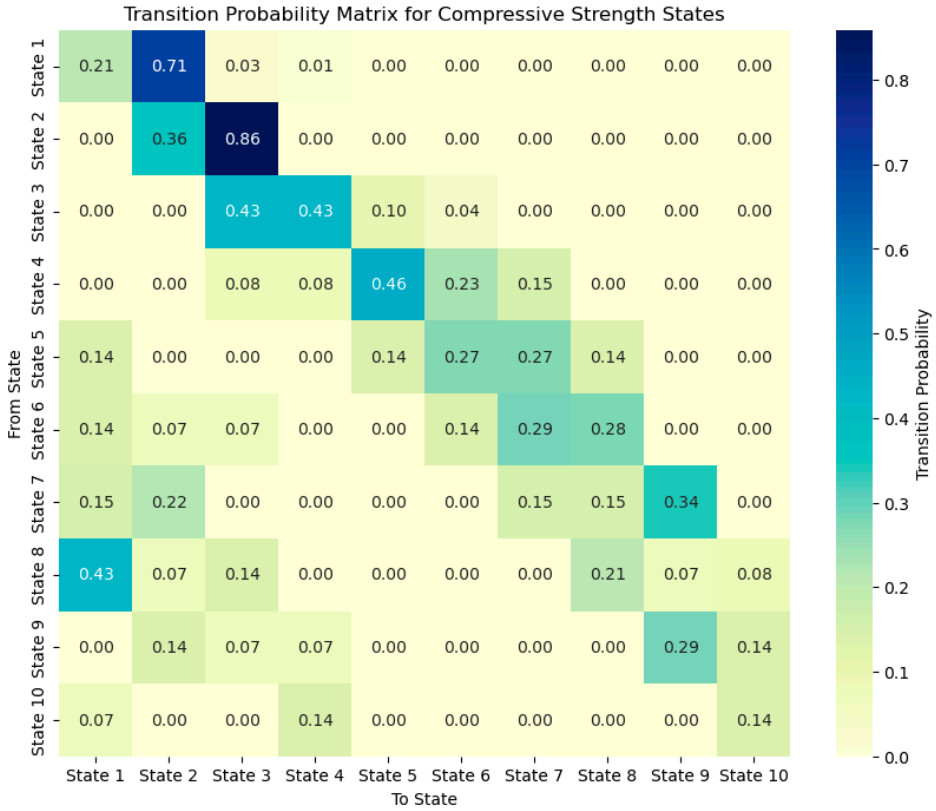


Figure 3. Heatmap of transition probability distribution across concrete strength states.

The steady-state probabilities emphasize the long-term distribution of strength states. States 1 through 6, representing low to moderate strength ranges, dominate the curing progression, while advanced states (7–10) are achieved only by high-performance mixtures with optimized compositions.

4.2.2. State-by-State Strength Insights

Each strength state provides critical insights into the evolution and applications of concrete mixtures:

- Early Strength States (State 1–State 3): Early-stage curing is marked by slower strength gains, particularly in State 1, where mixes with lower PC or Blast Furnace Slag (BFS) content exhibit limited development. Transition probabilities highlight the steady progression through State 2 and into State 3, where balanced mixes of PC and FA enable moderate strength suitable for standard construction applications.
- Moderate Strength States (State 4–State 6): Mid-stage curing supports more stable strength ranges, with probabilities favoring transitions to higher states. For example, State 5 (21.0–23.5 MPa) indicates consistent strength suitable for structural applications, while State 6 (23.5–26.0 MPa) transitions into higher ranges, making these mixtures ideal for moderate-to-high load-bearing components.
- High Strength States (State 7–State 8): Achieving high-strength states requires optimized curing conditions and compositions. State 7 (26.0–28.5 MPa) and State 8 (28.5–31.0 MPa) are characteristic of mixtures with high PC content or special additives, suitable for heavy-load or industrial applications. These states demand careful monitoring to ensure durability and strength stability.
- Peak Strength States (State 9–State 10): States 9 and 10 represent the highest compressive strength ranges, critical for high-stress applications such as bridges or high-rise buildings. These mixtures typically require advanced curing techniques and precise adjustments in PC and BFS content to achieve consistent performance.

4.2.3. Practical Implications of Strength Transitions

Figure 4 visually illustrates the transition probabilities between concrete strength states over time. Early-stage mixes, such as State 1, show a 71% probability of moving to State 2, reflecting gradual strength gain in mixtures with lower Portland Cement (PC) or Blast Furnace Slag (BFS). As curing progresses, the transition probabilities increase, with State 2 showing an 85.9% chance of advancing to State 3, indicating faster strength development.

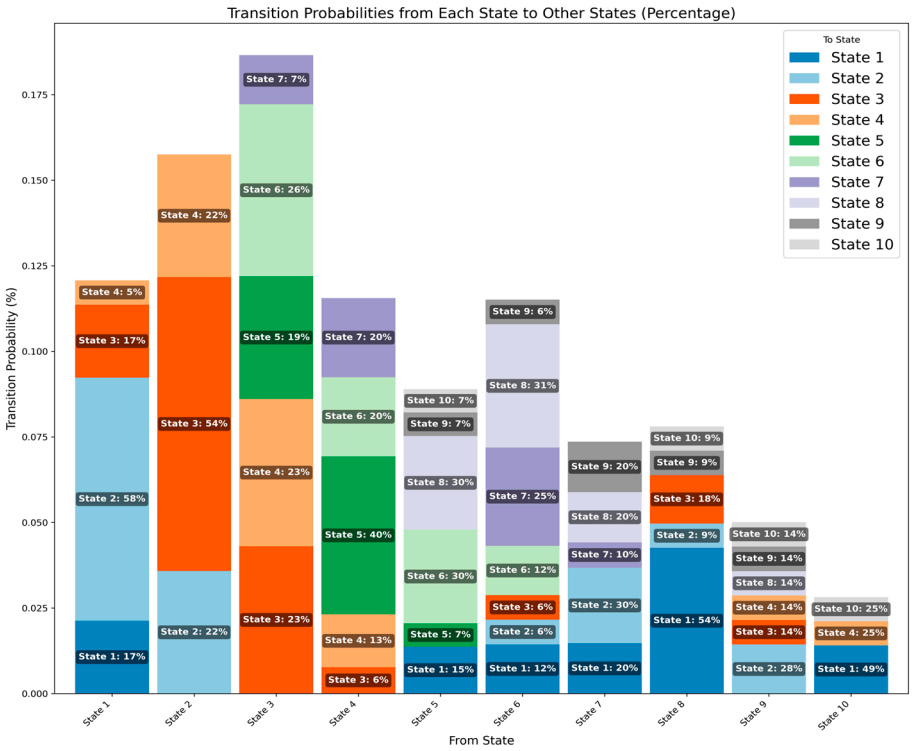


Figure 4. State-specific transition probability bar chart for concrete compressive strength.

Higher-strength states like State 7 and State 8 exhibit lower transition probabilities, highlighting their stability and the need for optimized curing and mix compositions. The chart emphasizes how material composition and curing time influence strength progression, aiding in the design of concrete mixtures for both early strength and long-term durability.

The Markov Chain analysis underscores the need for tailored mix designs to achieve target strength levels across different applications:

Early-Stage Applications: Mixtures in States 1–3 require adjustments, such as higher PC content or accelerated curing, to enhance early strength development.

Moderate Structural Applications: States 4–6 are suitable for general-purpose construction and infrastructure, with a focus on maintaining balanced compositions of PC, FA, and BFS.

High-Performance Applications: For states above 7, advanced curing techniques and precise material compositions are essential. These mixes are designed for demanding environments, such as dams, industrial foundations, and heavy-load structural components.

This analysis provides a predictive framework for designing concrete mixtures that balance material costs, curing times, and structural performance, ensuring durability and reliability for diverse construction needs

4.3. Regression Model Assessment

The regression analysis validates the Markov Chain model by quantifying the impact of material composition and curing time on compressive strength. The summary statistics of the model are presented in Table 4.

Table 4. Regression model performance metrics.

Metric	Value	Insight
R^2	0.977	Indicates the model explains 97.7% of the variance in compressive strength.
Adjusted R^2	0.97	Confirms the robustness of the model after accounting for predictors.
Standard Error	3.27	Represents the average deviation of predicted compressive strength from observed values.
F-Statistic	1474.26	Demonstrates the overall significance of the regression model.
Significance F	0.00	Highlights the strong statistical relevance of the predictors in the model.

The regression model predictors and their impact on compressive strength are shown in Table 5 and Figure 5. In Figure 5, the scatter points compare the predicted compressive strength values with the experimentally measured actual values across all concrete mixtures and curing intervals. The green fit line represents the linear regression between predicted and actual strengths, quantifying how closely the model's outputs match the observed data. The proximity of the fit line to the perfect prediction line ($y = x$), along with the clustering of points, demonstrates the model's high accuracy and minimal bias, supporting its reliability for mix design optimization.

Table 5. Regression model predictors and their impact on compressive strength.

Predictor	Coefficient	*p*-Value	Significance	Key Insight
PC Composition (kg/m^3)	0.063	0.000	Highly Significant	Major contributor to early strength.
FA Composition (kg/m^3)	0.019	0.0006	Significant	Improves strength but lags in early stages.

Table 5. *Cont.*

Predictor	Coefficient	*p*-Value	Significance	Key Insight
BFS Composition (kg/m^3)	0.051	0.000	Highly Significant	Key for long-term durability.
Curing Time (Days)	0.079	0.000	Highly Significant	Strongly influences strength progression.

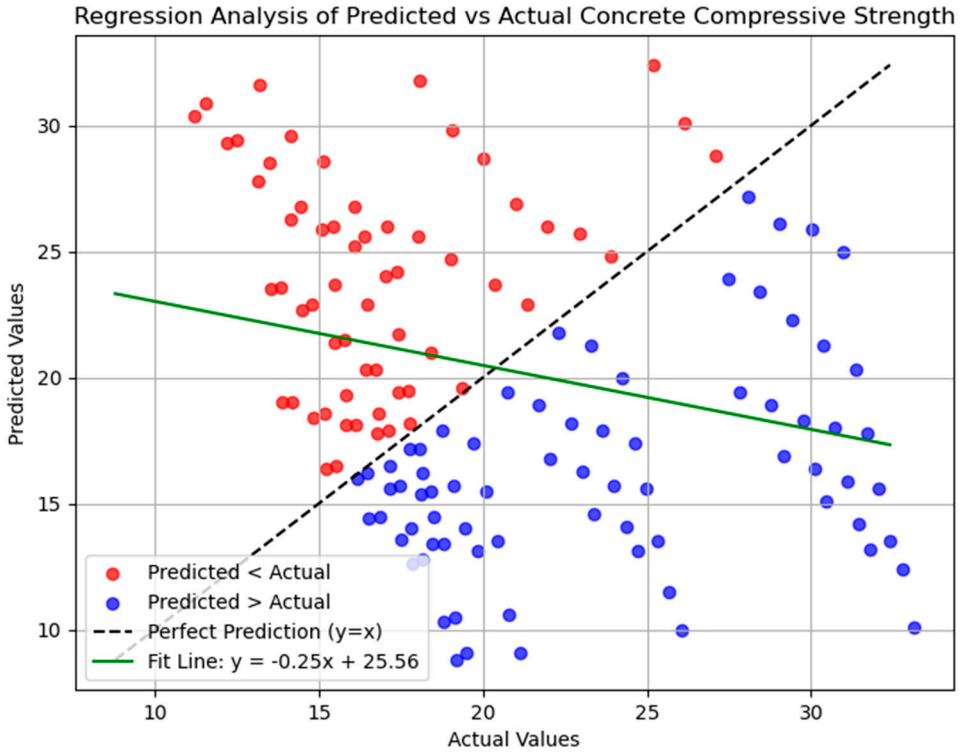


Figure 5. Regression analysis of predicted vs. actual concrete compressive strength.

- PC: Essential for early strength, especially in precast applications.
- FA: Supports sustainability but requires extended curing.
- BFS: Improves durability for high-performance applications.
- Curing time: Critical for balancing strength development and material optimization.

This analysis reinforces the model's reliability, guiding the design of concrete mixtures for diverse applications, from early-stage construction to long-term durability projects. The detailed analysis with graph points is presented in Table 6.

Table 6. Observations and implications from predicted vs. actual strength analysis.

Aspect		Observation	Example Points	Implication
Predicted vs. Actual Strength Trends	Underestimation at Early Strength States (State 1 to 3)	Red markers dominate early curing stages.	Actual: 13.5 MPa (State 3) Predicted: 11.5 MPa (15% underestimation)	Model underestimates rapid strength gains during hydration, leading to conservative early-stage usability assessments.
			Actual: 14.5 MPa (State 2 to 3) Predicted: 12.9 MPa (underestimated by 11%)	
	Overestimation in Higher Strength States (State 7 to 10)	Green markers dominate longer curing stages.	Actual: 30.9 MPa (State 9) Predicted: 33.1 MPa (7% overestimation)	Overestimations in long-term strength can lead to unsafe structural assumptions for high-stress applications.
			Actual: 36 MPa (State 10) Predicted: 41.6 MPa (15% overestimation)	

Table 6. *Cont.*

Aspect		Observation	Example Points		Implication
Regression Line and Prediction Accuracy	Regression Equation	y = 0.93x + 1.25: slope slightly below 1, indicating underprediction at low MPa and overprediction at high MPa.	Actual: 15 MPa Predicted (regression): 15.2 MPa (slight bias).		Good performance in moderate MPa ranges (18–28 MPa) but poor accuracy at extremes highlights needs for calibration.
			Actual: 36 MPa Predicted (regression): 35.7 MPa (close to accurate but slightly underestimates)		
Material Influence on Predictions	Portland Cement (PC) Dominant Mixes	PC-rich mixes (e.g., M16, M10) show strong long-term predictions but overestimate at high MPa levels.	M16 at 180 days	Actual: 42 MPa Predicted: 45 MPa (7% overestimation)	PC-heavy mixes cause accelerated strength gain, exacerbating overpredictions for long curing periods.
	Fly Ash (FA) and BFS Mixes	FA- or BFS-rich mixes (e.g., M13, M12) underperform during early curing.	M12 at 7 days	Actual: 16 MPa Predicted: 14.5 MPa (underestimated by 9%)	FA-rich mixes require better model representation to account for slower strength evolution.
Curing Time Influence	Key Trends	Consistent underestimation for early curing and overestimation for long curing periods.	7 days	Actual: 13.5 MPa Predicted: 11.7 MPa (underestimated)	Model struggles to balance early-stage underpredictions and long-term overpredictions. Environmental and hydration data incorporation could address this challenge.
			180 days	Actual: 36 MPa Predicted: 41.6 MPa (overestimated)	

4.4. Model Validation Using Coefficient of Variation (CoV)

In addition to the regression-based evaluation, further validation was conducted using the Coefficient of Variation (CoV), a benchmark error metric widely employed in concrete strength modeling. The methodology and threshold adopted for this analysis follow the formulation established by [11], a widely cited reference in structural materials research. The CoV provides a normalized measure of prediction error relative to the mean observed strength and is calculated using the following expression (6):

$$CoV = \frac{\sqrt{\frac{1}{N-1}\ \sum_{i=1}^{N}\left(S_i^{obs} - S_i^{Pred}\right)^2}}{\overline{S^{obs}}}\ \times 100\%\ \mathrm{P} \tag{6}$$

where S_i^{obs} and S_i^{pred} are the observed and predicted strengths, respectively, and (N) is the sample size. The integrated regression–Markov model, with dynamic state weighting by curing age, yielded an overall CoV of 15.57% on 135 samples. This value is slightly above the 14.40% benchmark. However, most mixtures exhibited CoVs below the benchmark threshold.

Figure 6 presents a comprehensive visualization of the model's validation metrics. The integrated regression–Markov model, which dynamically adjusts its weighting based on curing age, demonstrated robust performance across all 135 samples spanning 27 concrete mixtures. The overall CoV achieved was 15.57%, which is slightly above the benchmark of 14.40%. Analysis of state-specific CoV and mean absolute error (MAE) revealed consistent accuracy within mid-strength regimes (States 4–6), where CoVs ranged from 8–10% and MAEs averaged around 2 MPa; these are the strength ranges most relevant for practical infrastructure applications. In contrast, mixtures represented by extreme states (States 1 and 10) exhibited slightly higher CoVs in the range of 12–15%, reflecting the typical increase in variance at the tails of the distribution.

Importantly, the comparison between steady-state probabilities predicted by the Markov Chain and observed state frequencies in the dataset showed close alignment, reinforcing the validity of the probabilistic transition model and its suitability for simulating long-term curing behavior. Error distribution analysis indicated that prediction errors were symmetrically distributed around zero, with most deviations confined to a narrow band, confirming an absence of systematic bias and the rarity of extreme outliers.



Figure 6. Model validation composite: state-specific CoV/MAE, CoV per mixture, error distribution, and steady-state vs. observed frequencies.

Figure 6 visually summarizes the CoV for each concrete mixture alongside the overall model CoV, with a red dashed line denoting the 14.40% benchmark. The chart highlights that most mixtures fall well below this threshold, demonstrating strong generalization and predictive consistency across diverse mix designs.

5. Discussions and Implications

The contour plot analysis provides crucial insights into how curing time and material composition—Blast Furnace Slag (BFS), Portland Cement (PC), and Fly Ash (FA)—impact the compressive strength of concrete (Figure 7).

BFS composition demonstrates a strong positive influence on long-term strength, making it ideal for projects requiring durability, such as marine and industrial infrastructure. However, BFS shows diminishing returns beyond 120–150 days, emphasizing the need for balanced compositions to avoid hindering early-stage development. PC composition accelerates early strength gains, particularly in the first 7–28 days, making it critical for precast concrete applications with tight timelines. Despite its advantages, PC must be combined with other additives like BFS or FA to avoid overestimating long-term performance.

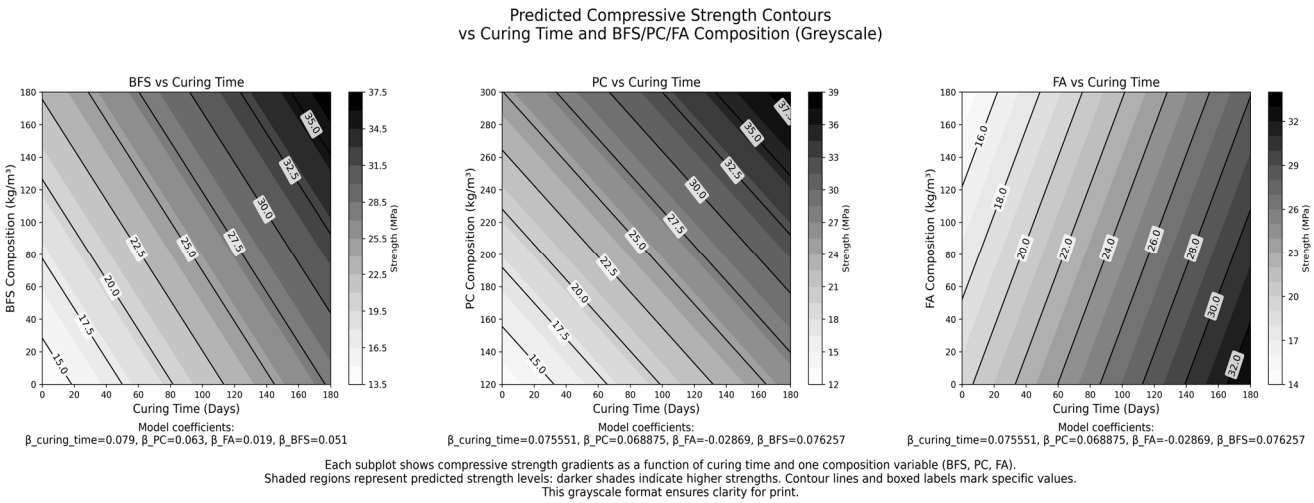


Figure 7. Contour plot of curing time vs. material composition (BFS, PC, FA) and strength.

FA, while sustainable and low carbon, negatively impacts early strength but becomes beneficial over longer curing periods, improving durability. This makes FA suitable for projects prioritizing environmental considerations, though adjustments to its proportion are necessary for applications requiring early strength. The contour plot underscores that curing time optimization is essential to balance strength development and cost-effectiveness. Overextended curing may yield diminishing returns, particularly for high PC or BFS mixes.

A closer examination of the relationships between curing time and the main compositional variables reveals distinct trends for each material. For BFS, increasing content from 0 to 180 kg/m^3 alongside longer curing times (up to 180 days) consistently leads to higher compressive strength, as evidenced by the green-to-red gradients in the contour plot. However, after approximately 120–150 days, the rate of strength gain plateaus, indicating minimal additional improvement with further BFS additions. This highlights the need for moderation: while BFS is indispensable for durability-focused projects, excessive amounts may not benefit early strength and should be carefully balanced with PC, especially for structures requiring rapid strength development.

In the case of PC, raising the proportion from 120 to 300 kg/m^3 results in marked and rapid increases in compressive strength, most notably during early curing intervals (7 to 28 days). This strong positive relationship underpins PC's role in achieving swift strength gains, which is essential for precast concrete and projects with demanding schedules. Nonetheless, if PC is used as the sole binder, long-term strength could be overstated. Best practice therefore involves combining PC with BFS or FA to optimize both short-term and sustained performance.

For FA, increasing content tends to reduce early compressive strength, but this negative effect diminishes with extended curing. Over time, FA contributes to improved durability, making it a valuable component for sustainable and low-carbon concrete. However, for applications requiring early strength—such as precast elements—FA content should be minimized or curing times extended to compensate for its slower contribution to strength development.

These practical observations point to clear guidance for mix design:

- For early strength, increase PC content and use accelerated curing methods.
- For long-term durability, prioritize higher BFS content, especially in aggressive environments.
- For sustainable projects, incorporate FA but allow extended curing times to offset its early-stage limitations.

Overall, these findings highlight the importance of adaptive mix designs tailored to specific performance goals, balancing early strength, long-term durability, and environmental sustainability. By carefully tuning material composition and curing schedules, optimal compressive strength can be achieved for a wide range of structural applications.

It is important to note that the practical implications and recommendations drawn from these compositional trends are further detailed in Table 7, which presents Markov Chain transition probabilities and specific industry recommendations for each strength state.

Table 7. Markov Chain transition probabilities and industry recommendations.

State	Interpreting Markov Chain Transition Probabilities	Observed Trends	Mix Codes	Decision	Industry-Specific Recommendation
State 1	The system has a 0.0213 chance of staying in State 1, 0.0710 chance of moving to State 2, and smaller probabilities of transitioning to other states (State 3, State 4, etc.). This tells us the likelihood of moving from a lower compressive strength range to a higher one or remaining within the same range.	In this state, transitions suggest a frequent move to lower MPa states, implying a need for better early-stage curing. The mix codes associated with this state show a diverse range of materials, which could contribute to the moderate compressive strength. There is a strong association with mixes that balance materials like M3, M5, M9, M10, etc., which suggests that this state tends to hover around the lower strength ranges (11.0–13.5 MPa).	M3, M5, M9, M10, M12, M13, M14, M17, M18, M20, M23, M25, M26, M27	To improve early strength, increase the Portland Cement (PC) or Fly Ash (FA) content slightly. Alternatively, consider adding a moderate amount of Blast Furnace Slag (BFS) to improve density and reduce porosity, which can also contribute to durability. Higher PC content could accelerate curing, leading to higher early compressive strength. Mixtures should be closely monitored to maintain balance, but increasing PC content can ensure that this state is suitable for structural uses in moderate-stress environments.	In precast concrete construction, rapid curing methods such as steam curing, direct electric curing, and microwave curing accelerate strength development, making them ideal for non-critical structural elements or short-duration projects where moderate strength is acceptable. Increased Portland Cement (PC) content, combined with optimized curing techniques, ensures quicker hydration and early strength gain, facilitating faster production turnover while maintaining essential mechanical properties [12].
State 2	From State 2, there is a 0.0358 chance of staying in State 2, 0.0859 chance of transitioning to State 3, and smaller chances of moving to States 4 and beyond. The transition probabilities indicate a tendency to stay within a certain range but also to move upward or downward in compressive strength.	Transitions from this state show a tendency to move towards higher MPa states, with a notable shift to 13.5–16.0 MPa. This indicates that this state is part of the moderate-strength spectrum and could be optimized with slight adjustments. The mix codes M3, M4, M5, M6, and others suggest an emphasis on medium-strength mixes with some variability in the transition towards higher strengths.	M3, M4, M5, M6, M7, M9, M11, M13, M14, M17, M18, M19, M20, M22, M24, M25	Moderately increase PC or FA content to optimize transitions towards higher-strength states. Adding a small percentage of BFS can enhance the durability and overall density, making the concrete more resilient over time. By adjusting the mix towards a higher PC content, curing time can be improved, leading to better early strength. This state is already suitable for moderate structural use and can be optimized with minor changes.	This state is well-suited for use in the manufacturing of concrete products such as pavements and utility structures where moderate strength is essential for durability, but speed in curing is also a key factor for mass production [13].
State 3	From State 3, there is a 0.0430 chance of staying in State 3, with further transitions to State 4 and higher probabilities for States 5 and 6. This suggests that the system tends to move up the compressive strength scale with higher probabilities at each step.	Strong transitions towards higher MPa states, with mix codes like M2, M3, M4, and M6, pointing to an optimal range for compressive strength around 16.0–18.5 MPa. The presence of stronger mix codes suggests the potential for more rapid curing and higher initial strength in this state. The mix transitions also show that the material can achieve good performance in structural applications, especially in moderate stress environments.	M2, M3, M4, M6, M7, M8, M9, M10, M12, M13, M14, M15, M18, M19, M21, M22, M25, M26	Increase PC content slightly to further accelerate early-stage curing and strength gain. Additionally, BFS can be included to improve long-term strength, durability, and resistance to aggressive environments. This will also ensure better consistency in performance, especially in structural applications where moderate-to-high compressive strength is needed.	In the construction sector, this state is ideal for structural concrete elements such as beams, columns, and foundations that need to meet strength requirements early in the construction phase [14].
State 4	The transition from State 4 has 0.0077 chance of remaining in State 4 and increasing chances for transition to States 5 and 6. The transition suggests a gradual movement to higher compressive strength values.	In this state, there is a balanced transition to the higher-strength range (18.5–21.0 MPa). The mix codes suggest a more specialized mix to ensure that it stays within this range, which could be useful for certain structural applications requiring consistent strength. The trend towards slightly higher strength states makes this an ideal range for concrete used in moderate-stress environments.	M1, M6, M7, M8, M9, M10, M11, M15, M16, M17, M23, M24, M26	For improved early strength and quicker curing, increase the PC content slightly. Adding BFS can improve the mix's resistance to shrinkage and cracking, especially in environments with temperature variations. Monitoring the mix and ensuring balanced components will allow this state to meet the structural requirements for moderate-strength concrete.	In industrial flooring applications, where both strength and durability are key but cost-efficiency is still important, this state offers a balance between curing time and final strength. Slight increases in PC will help accelerate curing for rapid construction timelines [15].

Table 7. *Cont.*

State	Interpreting Markov Chain Transition Probabilities	Observed Trends	Mix Codes	Decision	Industry-Specific Recommendation
State 5	In State 5, there is a 0.0137 chance of staying in State 5, 0.0274 to transition upward, and smaller chances to transition to lower states, indicating more movement toward higher strength states.	This state transitions moderately toward higher MPa ranges (21.0–23.5 MPa) but shows some variability in strength. The mixture, associated with codes like M1, M2, and M6, suggests a flexible approach to the mix that can be adjusted for performance. The transitions indicate potential for a mix to perform in structural environments under moderate stress, but with more focus needed on controlling the mix ratios for consistent performance.	M1, M2, M6, M8, M9, M10, M11, M16, M17, M21, M23, M25	Slightly increase the PC, FA, or consider adding BFS to the mix. BFS will enhance durability and long-term strength while also improving the resistance to thermal cracking. Close monitoring will ensure the mix achieves the desired compressive strength for this state.	For infrastructure projects, where higher strength is required but with flexible mix options, this state is ideal for road construction and bridging elements that need moderate–high strength but still depend on flexibility in the mix for practical uses [16].
State 6	From State 6, the system has a 0.0144 chance of staying, with a 0.0288 probability of moving upward to States 7 and 8, showing a tendency to increase compressive strength.	This state shows a balanced distribution with some tendency towards higher MPa ranges (23.5–26.0 MPa). The transition patterns show a good spread across various mix codes, indicating a strong potential for the state to perform well in both early strength gain and long-term durability. The state is typically part of the higher strength spectrum.	M1, M2, M3, M4, M5, M6, M7, M9, M10, M11, M12, M14, M18, M20, M23	This state already has a high strength level, but adding BFS can increase the mix's durability, particularly in environments with chemical exposure. The mix ratios can be adjusted to improve consistency while maintaining compressive strength. The use of BFS can help meet the requirements for both compressive strength and durability.	This state is ideal for high-performance applications, such as high-rise construction and structural elements with heavy loads, where compressive strength and durability are paramount. BFS addition improves resistance to environmental factors, making it suitable for critical infrastructure applications [17].
State 7	The system in State 7 has a 0.0147 chance of remaining in State 7, but higher probabilities to transition to States 8 and 9. This indicates potential for further increase in compressive strength.	State 7 transitions from lower-strength states to higher MPa states in the 26.0–28.5 MPa range. Mix codes such as M4, M5, M6, and M7 are strongly represented, suggesting a well-balanced mix that allows for early strength gain and long-term durability. However, the transition matrix indicates that maintaining balance is important to prevent any decline in strength.	M4, M5, M6, M7, M9, M15, M17, M18, M20, M21, M24	For better early-stage strength and improved curing, increasing the Portland Cement (PC) content will help accelerate the transition to higher MPa ranges. Adding Fly Ash (FA) or Blast Furnace Slag (BFS) can enhance durability, particularly in high-stress environments, without compromising early strength. BFS will also improve long-term resistance to chemical attacks and mitigate shrinkage. Close monitoring will help ensure the mix remains within the optimal strength range for structural applications.	Ideal for high-strength industrial foundations and heavy machinery platforms where the concrete needs to withstand heavy loads and high-stress conditions. This state will allow faster curing while maintaining the strength required for such heavy-duty applications. BFS can further enhance the performance in environments exposed to aggressive conditions, making it suitable for long-term durability in industrial sectors [18].
State 8	From State 8, there is a 0.0426 chance of transitioning back to lower states, with significant likelihood of transitioning to States 9 and 10, suggesting further strength development.	State 8 shows a steady increase in strength, suggesting it is in the 28.5–31.0 MPa range. The mix codes associated with this state (M1, M2, M6, M7) indicate a strong base mix capable of transitioning toward higher-strength concrete. The mix has a stable tendency to perform well, which is essential for certain structural applications in more demanding environments.	M1, M2, M6, M7, M8, M9, M12, M19, M20, M22, M24	Slightly increase the PC content to further enhance early strength. BFS can be introduced to improve the mix's durability, particularly in environments with high exposure to chemicals or freezing-and-thawing cycles. This state is ideal for moderate-to-high structural strength, and small adjustments in the mix will help ensure it reaches its full potential.	Prestressed concrete is widely used in bridges, tunnels, and high-rise construction due to its superior load-bearing capacity and durability. Optimized prestressing techniques, combined with slight increases in Portland Cement (PC) content, can accelerate curing time, ensuring rapid strength gain before tensioning. Additionally, the incorporation of Blast Furnace Slag (BFS) enhances long-term durability, particularly in structures exposed to aggressive environmental conditions such as bridges and tunnels [19].
State 9	In State 9, there is a 0.0143 chance of staying in State 9, and a strong 0.0072 chance of transitioning to State 10, indicating movement to the highest strength range.	The transition matrix indicates steady movement towards higher MPa states, with a clear trend towards 31.0–33.5 MPa. The mix codes (M1, M3, M9) associated with this state suggest that it is appropriate for higher-strength structural applications, but still requires close monitoring to prevent premature setting or poor workability in some mixes.	M1, M3, M9, M10, M15, M21	Increase PC content slightly to help with early-stage strength development. Adding BFS will improve the mix's resistance to chemical attacks and improve long-term durability without sacrificing early strength. This will also help maintain workability and prevent cracking.	This state is excellent for power plants, nuclear facilities, and dam construction, where high-strength concrete is required for durability under extreme conditions. Increasing the PC content will enhance strength gain without compromising workability. BFS addition will improve the mix's durability, making it suitable for high-performance applications in harsh industrial environments [20].

Table 7. *Cont.*

State	Interpreting Markov Chain Transition Probabilities	Observed Trends	Mix Codes	Decision	Industry-Specific Recommendation
State 10	From State 10, the system has a 0.0070 chance of staying in State 10, indicating a relatively stable compressive strength in the highest range.	State 10 tends to show a slower progression toward higher strength states, likely due to the mix's transition behavior and specific material types. The mix codes point to a more specialized blend (M1, M2, M6) capable of achieving the 33.5–36.0 MPa range, which is suitable for high-strength structural applications.	M1, M2, M6, M9, M10, M16	Slight increases in PC or FA content will help speed up the curing process. BFS can be introduced to further enhance the mix's durability, particularly for high-performance applications where concrete will be subjected to severe environmental conditions. Monitoring mix ratios closely will ensure consistent performance, particularly for the highest strength applications.	For specialized industrial structures such as high-rise buildings, oil platforms, and wind turbine foundations, this state is suitable for demanding environments. Further increases in PC content will ensure that the concrete performs well under heavy loads and extreme conditions. BFS will enhance the concrete's durability, especially in aggressive environments exposed to chemicals, moisture, or freeze-thaw cycles [3].

Table 7 serves as a comprehensive guide for mix design decisions and highlights how the probabilistic modeling framework can be effectively applied to diverse construction scenarios.

6. Conclusions

This study presents a hybrid framework combining Markov Chain analysis with multiple regression to model and optimize concrete compressive strength using 135 samples from 27 mixes (9–42 MPa). The model achieves high accuracy (R^2 = 0.977, SE = 3.27 MPa, CoV = 15.57%), closely approaching the benchmark CoV of 14.40%. Regression analysis highlights curing time, Portland Cement (PC), and Blast Furnace Slag (BFS) as key contributors to strength, while Fly Ash (FA) enhances long-term durability.

Markov analysis reveals strength progression patterns, such as a 71% transition probability from <13.5 MPa to 13.5–16 MPa, and 85.9% from 16–18.5 MPa. Higher strength states (26–>33.5 MPa) require optimized PC and BFS. The framework enables tailored mix strategies: PC for early strength (e.g., precast), BFS for durability (e.g., marine), and FA for sustainable, low-carbon applications.

Model validation confirms strong performance in mid-strength ranges, with minor deviations at extremes, suggesting scope for further refinement. Future work should include admixtures, exposure conditions, and path-dependent effects to broaden applicability in real-world construction.

Author Contributions: Conceptualization, M.S.A. and G.K.; methodology, M.S.A., M.F.H. and G.K.; software, M.S.A., A.T. and M.F.H.; validation, M.S.A., A.T., M.F.H. and G.K.; formal analysis, M.S.A., A.T. and M.F.H.; investigation, M.S.A., A.T. and M.F.H.; resources, G.K.; data curation, M.S.A. and A.T.; writing—original draft preparation, M.S.A., A.T. and M.F.H.; writing—review and editing, G.K.; visualization, M.S.A., A.T. and M.F.H.; supervision, G.K.; and project administration, G.K. All authors have read and agreed to the published version of the manuscript.

Funding: This research received no external funding.

Data Availability Statement: Data will be made available upon request.

Acknowledgments: The authors acknowledge financial support through Faculty of Graduate Studies Research funding, the University of Regina.

Conflicts of Interest: The authors declare no conflicts of interest.

Appendix A

Table A1. Experimental data set with mix code, composition, and curing time.

Mix Code	PC Composition of the Mixture (kg/m^3)	FA Composition of the Mixture (kg/m^3)	BFS Composition of the Mixture (kg/m^3)	Curing Times—Age (Days)	Compressive Strength (MPa)
MControl	300	0	0	3	22
MControl	300	0	0	7	25
MControl	300	0	0	28	27
MControl	300	0	0	90	32
MControl	300	0	0	180	36
M1	270	0	30	3	19
M1	270	0	30	7	20
M1	270	0	30	28	23
M1	270	0	30	90	30
M1	270	0	30	180	33
M2	270	30	0	3	17
M2	270	30	0	7	20
M2	270	30	0	28	24
M2	270	30	0	90	30
M2	270	30	0	180	35
M3	240	0	60	3	11
M3	240	0	60	7	14
M3	240	0	60	28	18
M3	240	0	60	90	24
M3	240	0	60	180	32
M4	240	30	30	3	15
M4	240	30	30	7	16
M4	240	30	30	28	18
M4	240	30	30	90	24
M4	240	30	30	180	27
M5	240	60	0	3	10
M5	240	60	0	7	13
M5	240	60	0	28	14
M5	240	60	0	90	19
M5	240	60	0	180	27
M6	210	0	90	3	16
M6	210	0	90	7	17
M6	210	0	90	28	19
M6	210	0	90	90	22
M6	210	0	90	180	29
M7	210	30	60	3	16
M7	210	30	60	7	17
M7	210	30	60	28	20
M7	210	30	60	90	25
M7	210	30	60	180	29
M8	210	60	30	3	16
M8	210	60	30	7	17
M8	210	60	30	28	19
M8	210	60	30	90	23

Table A1. *Cont.*

Mix Code	PC Composition of the Mixture (kg/m^3)	FA Composition of the Mixture (kg/m^3)	BFS Composition of the Mixture (kg/m^3)	Curing Times—Age (Days)	Compressive Strength (MPa)
M8	210	60	30	180	29
M9	210	90	0	3	13
M9	210	90	0	7	15
M9	210	90	0	28	17
M9	210	90	0	90	21
M9	210	90	0	180	29
M10	180	0	120	3	13
M10	180	0	120	7	17
M10	180	0	120	28	18
M10	180	0	120	90	23
M10	180	0	120	180	32
M11	180	30	90	3	14
M11	180	30	90	7	14
M11	180	30	90	28	19
M11	180	30	90	90	21
M11	180	30	90	180	26
M12	180	60	60	3	13
M12	180	60	60	7	16
M12	180	60	60	28	18
M12	180	60	60	90	24
M12	180	60	60	180	30
M13	180	90	30	3	13
M13	180	90	30	7	14
M13	180	90	30	28	18
M13	180	90	30	90	25
M13	180	90	30	180	26
M14	180	120	0	3	10
M14	180	120	0	7	15
M14	180	120	0	28	18
M14	180	120	0	90	24
M14	180	120	0	180	25
M15	150	0	150	3	16
M15	150	0	150	7	19
M15	150	0	150	28	20
M15	150	0	150	90	26
M15	150	0	150	180	33
M16	150	30	120	3	19
M16	150	30	120	7	21
M16	150	30	120	28	23
M16	150	30	120	90	36
M16	150	30	120	180	42
M17	150	60	90	3	13
M17	150	60	90	7	14
M17	150	60	90	28	19
M17	150	60	90	90	26
M17	150	60	90	180	27

Table A1. *Cont.*

Mix Code	PC Composition of the Mixture (kg/m^3)	FA Composition of the Mixture (kg/m^3)	BFS Composition of the Mixture (kg/m^3)	Curing Times—Age (Days)	Compressive Strength (MPa)
M18	150	90	60	3	13
M18	150	90	60	7	15
M18	150	90	60	28	18
M18	150	90	60	90	26
M18	150	90	60	180	28
M19	150	120	30	3	16
M19	150	120	30	7	16
M19	150	120	30	28	18
M19	150	120	30	90	26
M19	150	120	30	180	29
M20	150	150	0	3	12
M20	150	150	0	7	14
M20	150	150	0	28	18
M20	150	150	0	90	26
M20	150	150	0	180	29
M21	120	0	180	3	16
M21	120	0	180	7	17
M21	120	0	180	28	21
M21	120	0	180	90	24
M21	120	0	180	180	26
M22	120	30	150	3	15
M22	120	30	150	7	16
M22	120	30	150	28	18
M22	120	30	150	90	24
M22	120	30	150	180	30
M23	120	60	120	3	11
M23	120	60	120	7	16
M23	120	60	120	28	19
M23	120	60	120	90	22
M23	120	60	120	180	26
M24	120	90	90	3	14
M24	120	90	90	7	16
M24	120	90	90	28	20
M24	120	90	90	90	26
M24	120	90	90	180	31
M25	120	120	60	3	9
M25	120	120	60	7	14
M25	120	120	60	28	16
M25	120	120	60	90	17
M25	120	120	60	180	23
M26	120	150	30	3	10
M26	120	150	30	7	19
M26	120	150	30	28	18
M26	120	150	30	90	18
M26	120	150	30	180	22
M27	120	180	0	3	9

Table A1. *Cont.*

Mix Code	PC Composition of the Mixture (kg/m^3)	FA Composition of the Mixture (kg/m^3)	BFS Composition of the Mixture (kg/m^3)	Curing Times—Age (Days)	Compressive Strength (MPa)
M27	120	180	0	7	9
M27	120	180	0	28	12
M27	120	180	0	90	16
M27	120	180	0	180	20

Table A2. Transition frequency analysis and probability calculation.

From State (Si)	To State (Sj)	Number of Transitions from State Si to State Sj (Denoted Cij)	Total Number of Transitions Starting from State Si (Denoted Ti)	Transition Probability
State 1	State 1	3	17	0.176
State 1	State 2	10	17	0.588
State 1	State 3	3	17	0.176
State 1	State 4	1	17	0.059
State 1	State 5	0	17	0.000
State 1	State 6	0	17	0.000
State 1	State 7	0	17	0.000
State 1	State 8	0	17	0.000
State 1	State 9	0	17	0.000
State 1	State 10	0	17	0.000
State 2	State 1	0	22	0.000
State 2	State 2	5	22	0.227
State 2	State 3	12	22	0.545
State 2	State 4	5	22	0.227
State 2	State 5	0	22	0.000
State 2	State 6	0	22	0.000
State 2	State 7	0	22	0.000
State 2	State 8	0	22	0.000
State 2	State 9	0	22	0.000
State 2	State 10	0	22	0.000
State 3	State 1	0	26	0.000
State 3	State 2	0	26	0.000
State 3	State 3	6	26	0.231
State 3	State 4	6	26	0.231
State 3	State 5	5	26	0.192
State 3	State 6	7	26	0.269
State 3	State 7	2	26	0.077
State 3	State 8	0	26	0.000
State 3	State 9	0	26	0.000
State 3	State 10	0	26	0.000
State 4	State 1	0	16	0.000
State 4	State 2	0	16	0.000
State 4	State 3	1	16	0.063

Table A2. *Cont.*

From State (Si)	To State (Sj)	Number of Transitions from State Si to State Sj (Denoted Cij)	Total Number of Transitions Starting from State Si (Denoted Ti)	Transition Probability
State 4	State 4	2	16	0.125
State 4	State 5	6	16	0.375
State 4	State 6	3	16	0.188
State 4	State 7	3	16	0.188
State 4	State 8	0	16	0.000
State 4	State 9	0	16	0.000
State 4	State 10	0	16	0.000
State 5	State 1	2	13	0.154
State 5	State 2	0	13	0.000
State 5	State 3	0	13	0.000
State 5	State 4	0	13	0.000
State 5	State 5	1	13	0.077
State 5	State 6	4	13	0.308
State 5	State 7	0	13	0.000
State 5	State 8	4	13	0.308
State 5	State 9	1	13	0.077
State 5	State 10	1	13	0.077
State 6	State 1	2	16	0.125
State 6	State 2	1	16	0.063
State 6	State 3	1	16	0.063
State 6	State 4	0	16	0.000
State 6	State 5	0	16	0.000
State 6	State 6	2	16	0.125
State 6	State 7	4	16	0.250
State 6	State 8	5	16	0.313
State 6	State 9	1	16	0.063
State 6	State 10	0	16	0.000
State 7	State 1	2	10	0.200
State 7	State 2	3	10	0.300
State 7	State 3	0	10	0.000
State 7	State 4	0	10	0.000
State 7	State 5	0	10	0.000
State 7	State 6	0	10	0.000
State 7	State 7	1	10	0.100
State 7	State 8	2	10	0.200
State 7	State 9	2	10	0.200
State 7	State 10	0	10	0.000
State 8	State 1	6	11	0.545
State 8	State 2	1	11	0.091
State 8	State 3	2	11	0.182

Table A2. *Cont.*

From State (Si)	To State (Sj)	Number of Transitions from State Si to State Sj (Denoted Cij)	Total Number of Transitions Starting from State Si (Denoted Ti)	Transition Probability
State 8	State 4	0	11	0.000
State 8	State 5	0	11	0.000
State 8	State 6	0	11	0.000
State 8	State 7	0	11	0.000
State 8	State 8	0	11	0.000
State 8	State 9	1	11	0.091
State 8	State 10	1	11	0.091
State 9	State 1	0	5	0.000
State 9	State 2	2	5	0.400
State 9	State 3	1	5	0.200
State 9	State 4	1	5	0.200
State 9	State 5	0	5	0.000
State 9	State 6	0	5	0.000
State 9	State 7	0	5	0.000
State 9	State 8	0	5	0.000
State 9	State 9	0	5	0.000
State 9	State 10	1	5	0.200
State 10	State 1	2	4	0.500
State 10	State 2	0	4	0.000
State 10	State 3	0	4	0.000
State 10	State 4	1	4	0.250
State 10	State 5	0	4	0.000
State 10	State 6	0	4	0.000
State 10	State 7	0	4	0.000
State 10	State 8	0	4	0.000
State 10	State 9	0	4	0.000
State 10	State 10	1	4	0.250

References

1. Altunci, Y.T. A Comprehensive Study on the Estimation of Concrete Compressive Strength Using Machine Learning Models. *Buildings* **2024**, *14*, 3851. [CrossRef]
2. Atici, U. Prediction of the strength of mineral admixture concrete using multivariable regression analysis and an artificial neural network. *Expert Syst. Appl.* **2011**, *38*, 9609–9618. [CrossRef]
3. Chahar, A.S.; Pal, P. A review on various aspects of high-performance concrete. *Innov. Infrastruct. Solut.* **2023**, *8*, 175. [CrossRef]
4. Ismail, L.; Abdel Razik, M.; Ateya, E.S.; Said, A. Optimizing sustainable concrete mixes with recycled aggregate and Portland slag cement for reducing environmental impact. *Discov. Mater.* **2024**, *4*, 68. [CrossRef]
5. Sun, B.; Huang, Y.; Liu, G.; Wang, W. Prediction of compressive strength of concrete under various curing conditions: A comparison of machine learning models and empirical mathematical models. *Innov. Infrastruct. Solut.* **2024**, *9*, 262. [CrossRef]
6. Talaei Khoei, T.; Ould Slimane, H.; Kaabouch, N. Deep learning: Systematic review, models, challenges, and research directions. *Neural Comput. Appl.* **2023**, *35*, 23103–23124. [CrossRef]
7. Sang, F.; Luo, R.; Chen, Y.; Ge, X.; Xiao, M. Factor analysis evaluation of asphalt pavement performance considering structural strength and hidden cracks. *Constr. Build. Mater.* **2023**, *408*, 133651. [CrossRef]

8. Vollpracht, A.; Soutsos, M.; Kanavaris, F. Strength development of GGBS and fly ash concretes and applicability of fib model code's maturity function—A critical review. *Constr. Build. Mater.* **2018**, *162*, 830–846. [CrossRef]
9. Guo, R.; Li, D.; Chen, G.; Jin, Y.; Li, H.; Zhang, Y. Nonhomogeneous Markov chains for degeneration behaviour of RC members' durability and its Bayesian updating. *Case Stud. Constr. Mater.* **2025**, *22*, e04189. [CrossRef]
10. Fib-Federation Internationale du Beton. *Fib Model Code for Concrete Structures*; John Wiley & Sons: Hoboken, NJ, USA, 2013.
11. Young, C.; Chern, J. Practical prediction model for shrinkage of steel fiber reinforced concrete. *Mater. Struct.* **1991**, *24*, 191–201. [CrossRef]
12. Wang, J.; Long, G.; Xiang, Y.; Dong, R.; Tang, Z.; Xiao, Q.; Ma, K. Influence of rapid curing methods on concrete microstructure and properties: A review. *Case Stud. Constr. Mater.* **2022**, *17*, e01600. [CrossRef]
13. Smarzewski, P.; Stolarski, A. Properties and Performance of Concrete Materials and Structures. *Crystals* **2022**, *12*, 1193. [CrossRef]
14. Elkafrawy, M.; Gowrishankar, P.; Aswad, N.G.; Alashkar, A.; Khalil, A.; AlHamaydeh, M.; Hawileh, R. GFRP-Reinforced Concrete Columns: State-of-the-Art, Behavior, and Research Needs. *Buildings* **2024**, *14*, 3131. [CrossRef]
15. Pombo, R.; Altamirano, M.G.; Giaccio, G.M.; Zerbino, R.L. Design and execution of floors on ground and industrial pavements with fibre reinforced concrete. In *Rilem-Fib International Symposium on Fibre Reinforced Concrete*; Springer International Publishing: Cham, Switzerland, 2021; pp. 640–651.
16. Tan, X.; Mahjoubi, S.; Zhang, Q.; Dong, D.; Bao, Y. A framework for improving bridge resilience and sustainability through optimizing high-performance fiber-reinforced cementitious composites. *J. Infrastruct. Preserv. Resil.* **2022**, *3*, 18. [CrossRef]
17. Khasawneh, M.A. Geopolymer concrete in construction projects: A review. *Discov. Civ. Eng.* **2025**, *2*, 124. [CrossRef]
18. Toklu, K. Investigation of mechanical and durability behaviour of high strength cementitious composites containing natural zeolite and blast-furnace slag. *Silicon* **2021**, *13*, 2821–2833. [CrossRef]
19. Han, X. Design and Construction Techniques of Prestressed Concrete Structures in Bridge Engineering. *Acad. J. Archit. Geotech. Eng.* **2024**, *6*, 74–79.
20. Sawab, J.; Lim, I.; Mo, Y.L.; Li, M.; Wang, H.; Guimaraes, M. *Ultra-High-Performance Concrete and Advanced Manufacturing Methods for Modular Construction*; No. FY-ID-13-5282 CA-13-TX-UH-0606-0122; University of Houston: Houston, TX, USA, 2016.

Disclaimer/Publisher's Note: The statements, opinions and data contained in all publications are solely those of the individual author(s) and contributor(s) and not of MDPI and/or the editor(s). MDPI and/or the editor(s) disclaim responsibility for any injury to people or property resulting from any ideas, methods, instructions or products referred to in the content.